Theranostics

DOI: 10.1002/anie.201004867

Modular Polymer-Caged Nanobins as a Theranostic Platform with Enhanced Magnetic Resonance Relaxivity and pH-Responsive Drug Release**

Sang-Min Lee, Ying Song, Bong Jin Hong, Keith W. MacRenaris, Daniel J. Mastarone, Thomas V. O'Halloran, Thomas J. Meade, and SonBinh T. Nguyen**

Recent advances in nanoscience have spurred new developments in the field of theranostics (the combination of both therapeutic and diagnostic functionalities in a single system).[1] These nanoscale platforms possess improved pharmacokinetic profiles and targeting abilities for specific diseases.[2,3] Additionally, these integrated systems have been shown to selectively deliver therapeutic agents to target tissues while simultaneously monitoring biological responses to the therapy, thus providing important feedback in the treatment of highly heterogeneous diseases, particularly cancer.[4,5] Such concurrent evaluation of tumor response can be of crucial importance in clinical cancer therapy: treatments could be more successful if the prescribed regimens could be adjusted accordingly based on timely feedback.[6]

Magnetic resonance imaging (MRI) can provide detailed high-resolution, tomographic information of disease tissue in real time and in vivo. Hence, it has become a powerful diagnostic tool for detecting the stages of primary and recurrent solid tumors and for the assessment of suitable treatment regimens. Therefore, MRI is a suitable technique for use in conjunction with theranostic platforms for the post-treatment evaluation of solid tumors.

MRI studies are often conducted by using paramagnetic Gd^{III} complexes, which enhance the signal intensity by reducing the longitudinal relaxation time (T_1) of water protons close to the Gd^{III} center.[7] Despite the biomedical potential of MRI, the use of clinically available Gd^{III} contrast agents is hampered by their intrinsic low efficiency, which results in a need to administer high doses of contrast agents.[7] The conjugation of a large number of Gd^{III} ions to nanoscale structures, such as gold[8,9] and titanium oxide[10] nanoparticles, lipid nanoparticles,[11] and viral capsids,[12] has led to enhanced MR relaxivity. However, many of these systems do not have effective drug-loading capabilities, which limits their potential as theranostic platforms.

We have reported polymer-caged nanobins (PCNs) as a nanoscale delivery platform[13] that can be surface-modified with targeting groups by copper(I)-catalyzed 1,3-dipolar cycloaddition[14] in a facile manner. This platform is based on a liposomal template, which allows for the encapsulation of a high dose of small-molecule drugs by an ion-gradient-mediated (IGM) drug-loading process.[15] The polymer shell of PCN contains many terminal alkyne groups on the surface, hence azide-modified Gd^{III} complexes can be easily conjugated to drug-loaded PCNs to result in highly effective theranostic agents. The immobilization of Gd^{III} complexes on the surface of the PCN results in enhanced relaxivity per Gd^{III} ion caused by an increase in rotational correlation time (τ_R).[16,17] Additionally, the conjugation of a large number of Gd^{III} complexes to a single PCN leads to a high local concentration of contrast agents and significantly enhances the relaxivity per particle compared to small-molecule Gd^{III} agents.[9]

Herein, we demonstrate drug-loaded, gadolinium(III)-conjugated PCNs as a versatile theranostic platform with excellent drug uptake, high Gd^{III} loading, and enhanced MR relaxivity (both per Gd^{III} ion and per particle). The IGM drug-loading capability of the PCN system was expanded in this study to include gemcitabine (GMC, Gemzar Lilly, Greenfield, IN), which is a nucleoside analogue for an antimetabolite of deoxycytidine.[18] Clinically, GMC has been used as a first-line chemotherapeutic agent for non-small cell lung cancer,[19] pancreatic cancer,[20] metastatic breast cancer, and recurrent ovarian cancer.[21] Despite the clinical success of GMC, its short plasma half-life (9–13 minutes for human plasma)[22] and adverse toxicity such as myelosuppression greatly limit its chemotherapeutic efficacy.[19] By encapsulating GMC in PCN, the therapeutic index of GMC can be greatly improved because of the protection of the drug from renal clearance and prolonged circulation half-life.[23] In addition, the well-known enhanced permeation and retention (EPR) effect[24] will allow for preferential accumu-

[*] Dr. S.-M. Lee,[+] Dr. Y. Song,[+] Dr. B. J. Hong,[++] Dr. K. W. MacRenaris,[++] D. J. Mastarone, Prof. T. V. O'Halloran, Prof. T. J. Meade, Prof. S. T. Nguyen
Department of Chemistry and the Center of Cancer Nanotechnology Excellence, Northwestern University
2145 Sheridan Rd. Evanston, IL 60208-3113 (USA)
Fax: (+1) 847-491-7713
E-mail: tmeade@northwestern.edu
stn@northwestern.edu

[+] These authors contributed equally to this work.

[++] These authors contributed equally to this work.

[**] This work is financially supported by the NIH (NCI Center of Cancer Nanotechnology Excellence Grant U54 A119341 and Core Grant P30 A060553 to the Robert H. Lurie Comprehensive Cancer Center of Northwestern University and award number R01EB005866 from the National Institutes of Biomedical Imaging and Bioengineering). B.J.H. is partially supported by the National Research Foundation of Korea (NRF-2009-352-C00088).

Supporting information for this article, including the preparation of PCNs and other experimental procedures, is available on the WWW under http://dx.doi.org/10.1002/anie.201004867.

lation of the PCN-packaged drug in solid tumor tissues, thus facilitating the local drug uptake as well as release of drugs in the acidic environment of the tumor.[25] Indeed, our gadolinium(III)-conjugated, GMC-loaded PCNs (Gd^{III}–PCN_{GMC}) exhibit significant enhancement in r_1 relaxivity and pH-sensitive drug-release properties as a proof-of-concept theranostic platform (Figure 1).

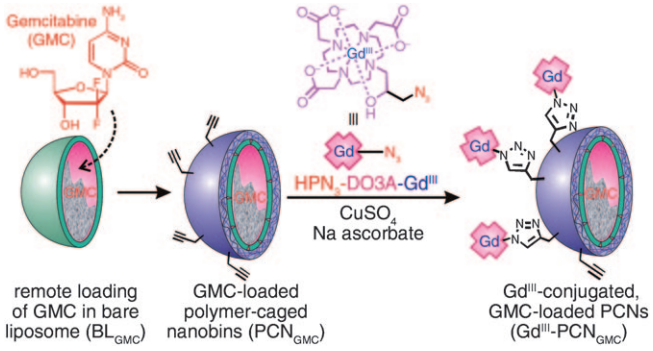

Figure 1. Preparation of gemcitabine-loaded, gadolinium(III)-conjugated polymer-caged nanobins (Gd^{III}–PCN_{GMC}) by copper(I)-catalyzed click ligation.

The mild basicity of GMC and its moderate lipophilicity[26] enable this drug to be remotely loaded into the core of a liposome by using the IGM drug-loading strategy. Therefore, GMC was added to a solution of bare liposomes, the cores of which contain ammonium sulfate (300 mM solution), and the resulting solution was incubated at 50 °C for 24 hours[27] before the unloaded GMC molecules were removed by gel filtration. The resulting GMC-loaded bare liposomes (BL_{GMC}, GMC/lipid = 0.25 mol/mol, GMC concentrations were measured by UV/Vis spectroscopy (see the Supporting Information, Figure S1) and lipid concentrations were measured by inductively coupled plasma optical emission spectrometry (ICP-OES)) were then modified with cholesterol-terminated poly(acrylic acid) (Chol-PAA, $M_n \approx 5{,}100$ Da) followed by in situ cross-linking with alkyne-functionalized diamine linkers[13] to prepare GMC-loaded PCNs (PCN_{GMC}) in which 50 % of the carboxyl groups of Chol-PAA were cross-linked.

The diameter of the resulting PCN_{GMC} was (108 ± 6) nm, as measured by dynamic light scattering (DLS; see the Supporting Information, Figure S2) and TEM (see the Supporting Information, Figure S3) with a zeta potential (ζ) of −(15.02±0.86) mV. As a large number of terminal alkyne groups is present on the surface of the PCN particles (ca. 150,000 groups per particle, 25 % of the total number of carboxyl groups of the Chol-PAA), gadolinium(III)-conjugated PCN_{GMC} with several Gd^{III}/lipid ratios were prepared by copper(I)-catalyzed click ligation[14] with [{10-(3-azido-2-hydroxypropyl)-1,4,7-tris(acetic acid) tetraazacyclododecane)} gadolinium(III)] (HPN_3-DO3A-Gd^{III}). After purification by gel filtration, Gd^{III}–PCN_{GMC} with final Gd^{III}/lipid ratios ranging between 0.032 and 0.45 were obtained (determined by ICP-OES, Table 1).

The aforementioned flexible strategy allows for a very high loading of Gd^{III} complexes per PCN (up to 45,000 Gd^{III} ions per particle) without significantly changing the diameter of the PCN (see the Supporting Information, Figure S2). As described above, because of the large number of available terminal alkynes, the loading of Gd^{III} complex can be increased further by higher percentages of cross-links or by the use of cross-linkers that possess multiple free alkynes.

Table 1: Relaxivities of Gd^{III}–PCNs at 60 MHz and 37 °C in water.

Agents	Gd^{III}/lipid	r_1 per Gd^{III} ion [$mM^{-1}s^{-1}$]	Gd^{III} ions per particle[a]	r_1 per particle [$mM^{-1}s^{-1}$]
DOTA–Gd^{III}	–	3.21	–	–
Gd^{III}–PCN_{GMC}1	0.032	11.3	3.2×10^3	36160
Gd^{III}–PCN_{GMC}2	0.11	14.5	1.1×10^4	165300
Gd^{III}–PCN_{GMC}3	0.24	15.0	2.4×10^4	352500
Gd^{III}–PCN_{GMC}4	0.45	15.9 (4.9)[b]	4.5×10^4	715500 (220500)[b]

[a] The number of lipid molecules per 100 nm liposome was assumed to be 10^5 based on data in Ref. [28, 29]. [b] Relaxivity measured at 300 MHz (7 T) and 25 °C in water.

To evaluate the relaxivity of each Gd^{III}–PCN_{GMC}, T_1 relaxation times were measured on a Bruker Minispec relaxometer at 37 °C and 60 MHz (1.41 T, which is comparable to the magnetic field strength of clinically used MR scanners).[30] The r_1 relaxivity value was calculated as the slope of a linear fit of $1/T_1$ (in s^{-1}) versus the concentration of Gd^{III} complexes (see the Supporting Information, Figures S4, S5, Table S1). The r_1 relaxivity was significantly increased with higher Gd^{III}/lipid ratios and reached a plateau of 15.9 $mM^{-1}s^{-1}$ at a Gd^{III}/lipid ratio of 0.45, which is approximately fivefold enhanced compared to that of DOTA–Gd^{III} (3.21 $mM^{-1}s^{-1}$)[17] (Table 1).

The enhanced relaxivity of Gd^{III}–PCNs is presumably a result of a longer rotational correlation time (τ_R) because of the anchoring of the Gd^{III} complexes on the polymer cages, which is consistent with the Solomon–Bloembergen–Morgan theory.[31] Given that approximately 10^5 lipid molecules are present in a 100 nm liposome particle,[28,29] a single Gd^{III}–PCN particle with a Gd^{III}/lipid ratio of 0.45 can exhibit a relaxivity of 715500 $mM^{-1}s^{-1}$ per particle at 60 MHz (220500 $mM^{-1}s^{-1}$ per particle at 300 MHz, Table 1). T_1-weighted MR images of Gd^{III}–PCN_{GMC} in solution were acquired at 7 T and 25 °C, thus showing a significant contrast enhancement relative to the DOTA–Gd^{III} platform (see the Supporting Information, Figure S6).

Drug-delivery vehicles with negligible cargo-release profiles often have low therapeutic potencies in both in vitro[32] and in vivo[33] trials. Hence triggered drug-release properties under specific conditions are important criteria in the design of efficient therapeutic and theranostic platforms. Given the known acidity in the tumor interstitium[25] and in the cellular endosomes,[34] acid sensitivity has been shown to be a good trigger for drug release from delivery vehicles in cancer therapy. As PCNs possess acid-triggered cargo-release characteristics because of their pH-responsive polymer shells,[35] the drug-release profiles of all samples of Gd^{III}–PCN_{GMC} were monitored at pH 5.0 and 37 °C and compared to those at physiological conditions (pH 7.4, 37 °C). To this end, Gd^{III}–

PCN_{GMC} was incubated in acetate (pH 5.0) or 4-(2-hydroxyethyl)-1-piperazineethanesulfonic acid (HEPES, pH 7.4) buffers (both contain 150 mM NaCl) and the drug-release kinetics were measured by comparing the GMC/lipid ratios in the remaining PCNs after purification by filtration. As expected, the release rates were clearly pH-dependent for Gd^{III}–PCN_{GMC} (Figure 2 and Table S2 in the Supporting Information): approximately 75% of GMC was released

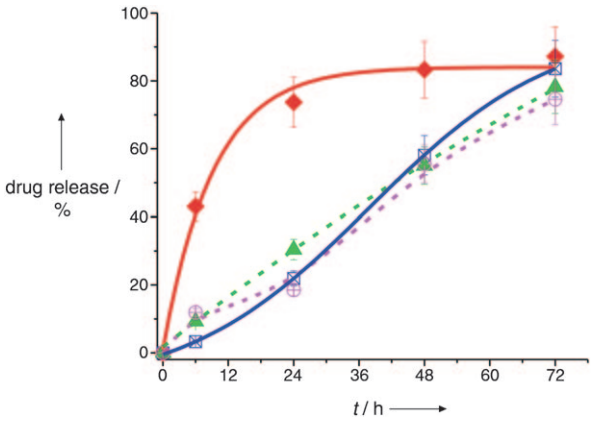

Figure 2. Time-dependent GMC-releasing profiles of bare liposome (BL_{GMC}) or Gd^{III}–PCN_{GMC} (Gd^{III}/lipid = 0.45) beneath either pH 5.0 or 7.4 and at 37°C (green triangles: BL_{GMC} at pH 5.0, open pink circles: BL_{GMC} at pH 7.4, red diamonds: Gd^{III}–PCN_{GMC} at pH 5.0, open blue squares: Gd^{III}–PCN_{GMC} at pH 7.4). The linear release profiles observed for BL_{GMC} are attributed to the moderate lipophilicity of GMC.

from Gd^{III}–PCN_{GMC}4 within the initial 24 hours and near-complete release was achieved within 48 hours. In comparison, under neutral conditions, approximately 20% and 60% of GMC were released from Gd^{III}–PCN_{GMC}4 within 24 hours and 48 hours, respectively. This release behavior of DOTA–Gd^{III}4 at pH 7.4 is similar to the release profile of BL_{GMC}, where no significant differences in release were observed at either pH 7.4 or 5.0 (Figure 2). This acid-sensitive drug-release property of DOTA–Gd^{III} demonstrated its excellent potential as a cancer theranostic agent.

The in vitro therapeutic potency of Gd^{III}–PCN_{GMC} was evaluated by using HeLa human cervical cancer cells (Figure 3; see the Supporting Information, Figure S7). Surprisingly, Gd^{III}–PCN_{GMC} exhibited significantly higher potency (half-maximal inhibitory concentration (IC_{50}) of 14.4 μM) than free GMC (IC_{50} of ca. 100 μM). This observation is attributed to the enhanced cellular uptake of the encapsulated drug, which can be internalized into the cell by endocytosis of the nanoscale delivery vehicles.[36] In contrast, the uptake of free GMC into HeLa cells can be relatively low, because GMC uptake is mostly mediated by human concentrative nucleoside transporters (hCNTs, trans-membrane proteins that normally mediate the cellular uptake of nucleosides[21]) such as hCNT1 and hCNT3, which are absent in HeLa cells.[37,38] Indeed, GMC has been shown to have very limited potency in HeLa cell lines[39] without the specific expression of target transporters.[40] Therefore, PCN encapsulation provides a new possibility for small-molecule nucleo-

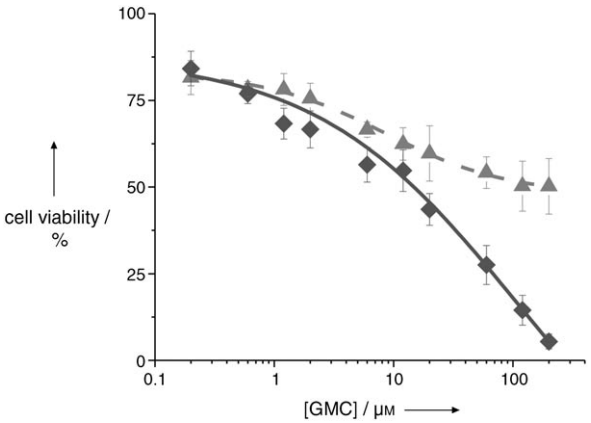

Figure 3. Plots of dose-responsive cell viability of HeLa cells exposed to free GMC (triangles) and Gd^{III}–PCN_{GMC} (diamonds; Gd^{III}/lipid = 0.45) after incubation for 72 h.

side-analogue drugs that confer cytotoxicity to cancer cells and lack the expression of specific target transporters. Once the encapsulated drugs have been taken up into the cell by endocytosis, the pH-sensitive polymer cage of PCN can destabilize the endosomal membrane under acidic conditions, thus leading to the rupture of endosomal vesicles.[41] Such a polymer-mediated membrane perturbation can substantially facilitate the delivery of drug molecules from the endosomes into the cytosol to result in enhanced therapeutic efficacy.

The aforementioned hypothesis is supported by quantification studies that show the enhanced cellular uptake of Gd^{III}–PCNs over DOTA–Gd^{III}. To determine the cellular internalization efficacy, HeLa cells were incubated for 24 hours in complete media, which contained either GMC-free Gd^{III}–PCNs or DOTA–Gd^{III} molecules. The cellular Gd^{III} uptake was determined by ICP-MS after washing three times with Dulbecco's modified phosphate-buffered saline (DPBS), followed by harvesting, centrifugation, supernatant removal, and further cell-pellet washing to remove any nonspecifically bound Gd^{III}–PCNs. The results show that the Gd^{III} uptake for cells incubated with Gd^{III}–PCNs (Gd^{III}/lipid = 0.45) is 30 to 70 times higher than that of cells treated with DOTA–Gd^{III} (Figure 4). This cellular uptake enhancement of Gd^{III}–PCNs was observed to be both dose- and time-dependent in both HeLa cells and noncancerous NIH/3T3 mouse fibroblast cells (see the Supporting Information, Figures S9, S10), thus suggesting a typical endocytosis-internalization mechanism.[42] The enhanced cellular uptake of Gd^{III}–PCNs compared to the corresponding small-molecule agents helps to explain the aforementioned enhanced potency of Gd^{III}–PCN_{GMC}.

In sharp contrast to Gd^{III}–PCN_{GMC}, drug-free Gd^{III}–PCNs show negligible cytotoxicity (see the Supporting Information, Figures S11, S12), even with their enhanced cellular uptake. Therefore, the conjugation of Gd^{III} complexes to PCNs provides not only a theranostic platform but also a highly efficient cellular-labeling agent that can be used for long-term cell tracking and lineage studies in vivo. The delivery and cellular contrast enhancement is an improvement compared to previously tested small-molecule contrast agents such as

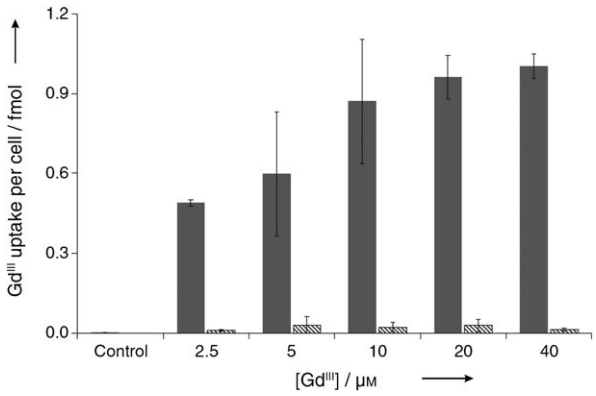

Figure 4. Concentration-dependent, cellular uptake profile of Gd^{III}–PCNs (Gd^{III}/lipid = 0.45, solid bars) compared to DOTA–Gd^{III} (shaded bars) by HeLa human cervical cancer cells. Cells were incubated in complete media, which contained Gd^{III}–PCNs or DOTA–Gd^{III} at given Gd^{III} concentrations for 24 h at 37 °C.

polyarginine because of the enhanced cellular uptake and minimal non-specific binding of PCNs.[43]

The enhanced cellular internalization of Gd^{III}–PCNs by endocytosis suggests the potential of these nanobins as noninvasive cell-tracking agents for MRI.[44] Indeed, the high uptake of Gd^{III}–PCNs was clearly reflected in the significant contrast enhancement observed in the T_1-weighted MR images of NIH/3T3 cells that were exposed to Gd^{III}–PCNs, compared to those of cells exposed to DOTA–Gd^{III} (Figure 5; see the Supporting Information, Table S3). Such an enhanced contrast was also observed in the T_1-weighted MR images of HeLa cells (see the Supporting Information, Figure S13, Table S4). Together with the improved therapeutic efficacy observed for Gd^{III}–PCN_{GMC}, these results demonstrate the promising potential of the Gd^{III}–PCN_{DRUG} platform as a cell-permeable theranostic agent.

In conclusion, we have demonstrated the versatility of unprecedented "clickable" polymer-caged nanobins for the simultaneous incorporation of high doses of Gd^{III}-based MRI contrast agents and an anticancer drug, gemcitabine, in a single delivery theranostic platform. The conjugation of a large number of Gd^{III} complexes to the surface of the PCN by copper(I)-catalyzed click ligation significantly enhanced the per Gd^{III} MR relaxivity, thus resulting in a very high relaxivity per particle.

Notably, the "nano-packaging" of gemcitabine inside the PCN circumvents the transporter-specific cellular membrane uptake pathway, which often limits the therapeutic effectiveness of nucleoside analogue drugs, thus making the combined Gd^{III}–PCN_{GMC} materials a much better theranostic agent than either of its components. Our PCN strategy, which involves Cu(I)-catalyzed click chemistry, is highly specific for tuning the Gd^{III}/GMC loading ratio (0.128 to 1.8). This aspect allows for the specific matching of the ratios of active drugs and MR contrast agents that can remedy the detrimental sensitivity and concentration mismatches between therapeutics and diagnostics in combined theranostic platforms.[1]

Besides the enhanced r_1 relaxivity reported herein, the most obvious benefit from attaching an imaging agent to a nanoscale drug delivery agent such as our PCN platform is the ability to verify if the drug delivery agent has reached its targeted diseased organs or tissues. Several other advantages are also apparent: firstly, if an MRI contrast agent can be co-delivered with a drug in a single nanoscale package that can target to a specific diseased site, a broader range of organs and tissues can be imaged beyond the current limited group of vasculature network, liver, and kidney.[45] Secondly, because nanoparticle delivery is quite specific in cancer chemotherapy, whether through the EPR effect or active targeting, a much smaller amount of the imaging agent is needed, thus lessening the material cost and any potential side effects that might be caused by the imaging agent. A third advantage of a theranostic platform such as our PCN is the macroscopic nature of the gadolinium(III)-functionalized polymer cage, which should result in an increased residence time for the Gd^{III} MRI contrast agent at the diseased site, allowing for long-term repeated imaging to evaluate the benefits of the treatment. As a consequence, the prescribed regimen can be adjusted in a timely fashion from ongoing feedback information and can allow for more successful treatment.

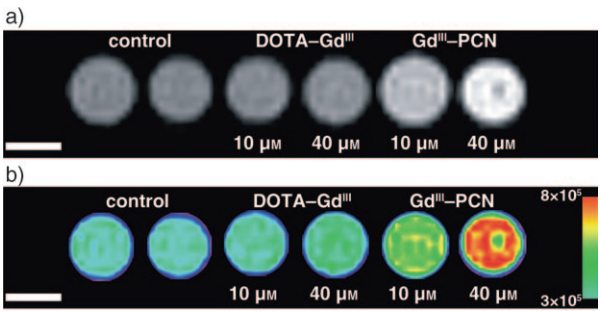

Figure 5. a) T_1-weighted MR image of NIH/3T3 mouse fibroblast cells incubated with solutions of Gd^{III}–PCNs (Gd^{III} concentrations: 10 μM and 40 μM, Gd^{III}/lipid = 0.39) and DOTA–Gd^{III} (Gd^{III} concentrations: 10 μM and 40 μM) for 24 h at 7 T (300 MHz) and 25 °C (TR/TE = 500/11 ms; TR = repetition time; TE = echo time). b) The corresponding image-intensity color map for panel a) where the maximum and minimum image intensities are shown in the calibration bar on the right-hand side. The scale bars at the bottom left corners in both images correspond to 1.0 mm.

Received: August 5, 2010
Published online: November 16, 2010

Keywords: antitumor agents · drug delivery · gadolinium · liposomes · magnetic resonance imaging

[1] J. R. McCarthy, *Nanomedicine* **2009**, *4*, 693 – 695.
[2] D. Peer, J. M. Karp, S. Hong, O. C. Farokhzad, R. Margalit, R. Langer, *Nat. Nanotechnol.* **2007**, *2*, 751 – 760.
[3] M. E. Davis, Z. Chen, D. M. Shin, *Nat. Rev. Drug Discovery* **2008**, *7*, 771 – 782.
[4] B. Sumer, J. Gao, *Nanomedicine* **2008**, *3*, 137 – 140.
[5] K. B. Hartman, L. J. Wilson, M. G. Rosenblum, *Mol. Diagn. Ther.* **2008**, *12*, 1 – 14.
[6] P. Therasse, S. G. Arbuck, E. A. Eisenhauer, J. Wanders, R. S. Kaplan, L. Rubinstein, J. Verweij, M. Van Glabbeke, A. T.

van Oosterom, M. C. Christian, S. G. Gwyther, *J. Natl. Cancer Inst.* **2000**, *92*, 205 – 216.
[7] J. L. Major, T. J. Meade, *Acc. Chem. Res.* **2009**, *42*, 893 – 903.
[8] C. Alric, J. Taleb, G. L. Duc, C. Mandon, C. Billotey, A. L. Meur-Herland, T. Brochard, F. Vocanson, M. Janier, P. Perriat, S. Roux, O. Tillement, *J. Am. Chem. Soc.* **2008**, *130*, 5908 – 5915.
[9] Y. Song, X. Xu, K. W. MacRenaris, X.-Q. Zhang, C. A. Mirkin, T. J. Meade, *Angew. Chem.* **2009**, *121*, 9307 – 9311; *Angew. Chem. Int. Ed.* **2009**, *48*, 9143 – 9147.
[10] P. J. Endres, T. Paunesku, S. Vogt, T. J. Meade, G. E. Woloschak, *J. Am. Chem. Soc.* **2007**, *129*, 15760 – 15761.
[11] J. C. Frias, K. J. Williams, E. A. Fisher, Z. A. Fayad, *J. Am. Chem. Soc.* **2004**, *126*, 16316 – 16317.
[12] A. Datta, J. M. Hooker, M. Botta, M. B. Francis, S. Aime, K. N. Raymond, *J. Am. Chem. Soc.* **2008**, *130*, 2546 – 2552.
[13] S.-M. Lee, H. Chen, T. V. O'Halloran, S. T. Nguyen, *J. Am. Chem. Soc.* **2009**, *131*, 9311 – 9320.
[14] V. V. Rostovtsev, L. G. Green, V. V. Fokin, K. B. Sharpless, *Angew. Chem.* **2002**, *114*, 2708 – 2711; *Angew. Chem. Int. Ed.* **2002**, *41*, 2596 – 2599.
[15] T. M. Allen, *Drugs* **1998**, *56*, 747 – 756.
[16] P. Caravan, *Chem. Soc. Rev.* **2006**, *35*, 512 – 523.
[17] Y. Song, E. K. Kohlmeir, T. J. Meade, *J. Am. Chem. Soc.* **2008**, *130*, 6662 – 6663.
[18] W. Plunkett, P. Huang, V. Gandhi, *Anti-Cancer Drugs* **1995**, *6*, 7 – 13.
[19] S. Noble, K. L. Goa, *Drugs* **1997**, *54*, 447 – 472.
[20] G. Friberg, H. Kindler, *Curr. Oncol. Rep.* **2005**, *7*, 186 – 195.
[21] J. Zhang, F. Visser, K. King, S. Baldwin, J. Young, C. Cass, *Cancer Metastasis Rev.* **2007**, *26*, 85 – 110.
[22] J. M. Reid, W. Qu, S. L. Safgren, M. M. Ames, M. D. Krailo, N. L. Seibel, J. Kuttesch, J. Holcenberg, *J. Clin. Oncol.* **2004**, *22*, 2445 – 2451.
[23] R. Moog, A. Burger, M. Brandl, J. Schüler, R. Schubert, C. Unger, H. Fiebig, U. Massing, *Cancer Chemother. Pharmacol.* **2002**, *49*, 356 – 366.
[24] H. Maeda, J. Wu, T. Sawa, Y. Matsumura, K. Hori, *J. Controlled Release* **2000**, *65*, 271 – 284.
[25] I. F. Tannock, D. Rotin, *Cancer Res.* **1989**, *49*, 4373 – 4384.
[26] F. Castelli, M. G. Sarpietro, M. Ceruti, F. Rocco, L. Cattel, *Mol. Pharmaceutics* **2006**, *3*, 737 – 744.
[27] G. Haran, R. Cohen, L. K. Bar, Y. Barenholz, *Biochim. Biophys. Acta Biomembr.* **1993**, *1151*, 201 – 215.
[28] H. G. Enoch, P. Strittmatter, *Proc. Natl. Acad. Sci. USA* **1979**, *76*, 145 – 149.
[29] T. M. Allen, C. B. Hansen, D. E. L. de Menezes, *Adv. Drug Delivery Rev.* **1995**, *16*, 267 – 284.
[30] P. Glover, R. Bowtell, *Nature* **2009**, *457*, 971 – 972.
[31] S. Zhang, M. Merritt, D. E. Woessner, R. E. Lenkinski, A. D. Sherry, *Acc. Chem. Res.* **2003**, *36*, 783 – 790.
[32] D. Smith, S. H. Clark, P. A. Bertin, B. L. Mirkin, S. T. Nguyen, *J. Mater. Chem.* **2009**, *19*, 2159 – 2165.
[33] S. Bandak, D. Goren, A. Horowitz, D. Tzemach, A. Gabizon, *Anti-Cancer Drugs* **1999**, *10*, 911 – 920.
[34] J. R. Casey, S. Grinstein, J. Orlowski, *Nat. Rev. Mol. Cell Biol.* **2010**, *11*, 50 – 61.
[35] S.-M. Lee, H. Chen, C. M. Dettmer, T. V. O'Halloran, S. T. Nguyen, *J. Am. Chem. Soc.* **2007**, *129*, 15096 – 15097.
[36] R. Savic, L. Luo, A. Eisenberg, D. Maysinger, *Science* **2003**, *300*, 615 – 618.
[37] J. García-Manteiga, M. Molina-Arcas, F. J. Casado, A. Mazo, M. Pastor-Anglada, *Clin. Cancer Res.* **2003**, *9*, 5000 – 5008.
[38] M. L. Clarke, V. L. Damaraju, J. Zhang, D. Mowles, T. Tackaberry, T. Lang, K. M. Smith, J. D. Young, B. Tomkinson, C. E. Cass, *Mol. Pharmacol.* **2006**, *70*, 303 – 310.
[39] M. Ogawa, H. Hori, T. Ohta, K. Onozato, M. Miyahara, Y. Komada, *Clin. Cancer Res.* **2005**, *11*, 3485 – 3493.
[40] P. D. Dobson, D. B. Kell, *Nat. Rev. Drug Discovery* **2008**, *7*, 205 – 220.
[41] M.-A. Yessine, J.-C. Leroux, *Adv. Drug Delivery Rev.* **2004**, *56*, 999 – 1021.
[42] L. Luo, J. Tam, D. Maysinger, A. Eisenberg, *Bioconjugate Chem.* **2002**, *13*, 1259 – 1265.
[43] M. J. Allen, K. W. MacRenaris, P. N. Venkatasubramanian, T. J. Meade, *Chem. Biol.* **2004**, *11*, 301 – 307.
[44] K. Bhakoo, C. Chapon, J. Jackson, W. Jones in *Modern Magnetic Resonance* (Ed.: G. A. Webb), **2006**, pp. 879 – 890.
[45] S. Aime, P. Caravan, *J. Magn. Reson. Imaging* **2009**, *30*, 1259 – 1267.

